BOND JOINT STRENGTH DEGRADATION DUE TO INTERLAYER INCLUSIONS IN LAMINATED COMPOSITE ADHERENT

Akash Pisharody
Phd Candidate
Baylor University, Waco, Texas, USA

Contents

Introduction

- Adhesive bonding advantages [1]
  - Weight efficient
  - Cost effective
  - Versatile
  - Corrosion resistant
- Types of joints [2]
  - Single Lap
  - Double Lap
  - Scarf
  - Stepped
  - T-Joints
- Carbon fiber Composites [2]
  - Being extensively used in aerospace and automobile industries
  - Higher strength to weight ratios
  - Challenges in joining composites

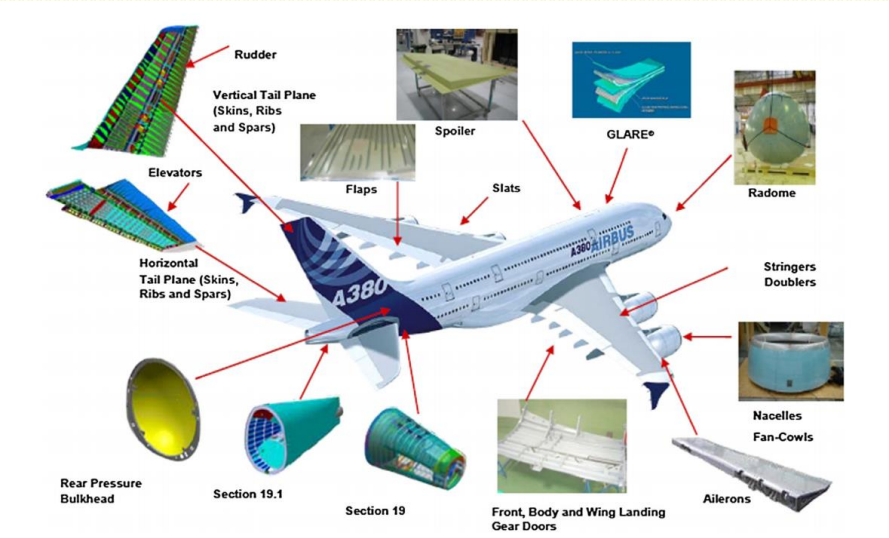

Fig.1 Usage of adhesive bonding in Airbus A380 [1]

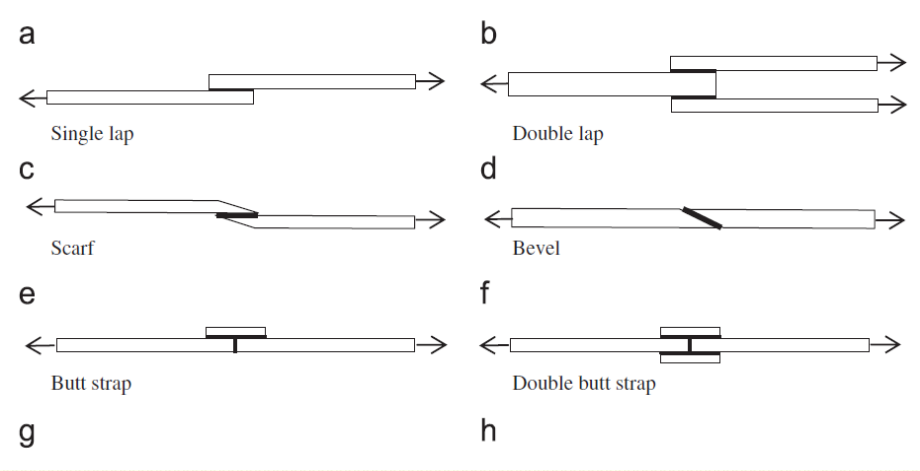

Fig.2 Common configurations in adhesive lap joint [2]

Introduction

- Single lap joints
  - Widely used for their efficiency, simplicity and ability to produce a condition of mixed loading [2].
  - Deformation of single lap joints causes shear and peel stresses.
  - Single lap joints are used as the primary test vehicle for this study

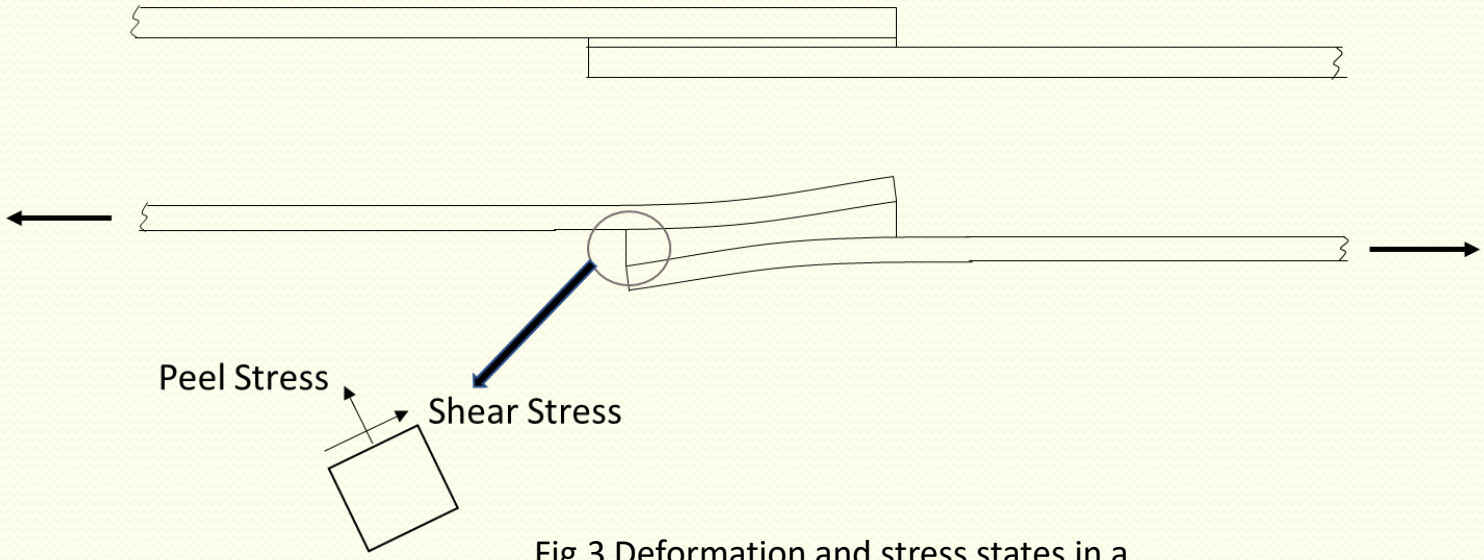

Fig.3 Deformation and stress states in a Single Lap Joint

Introduction

- Failure Modes [2]
  - Adhesive
  - Cohesive
  - Fiber-tear
  - Adherent failure
- Defects [3]
  - Voids
  - Inclusions (Foreign objects)
  - Cracks
  - Local lack of adhesion (Kissing bonds)

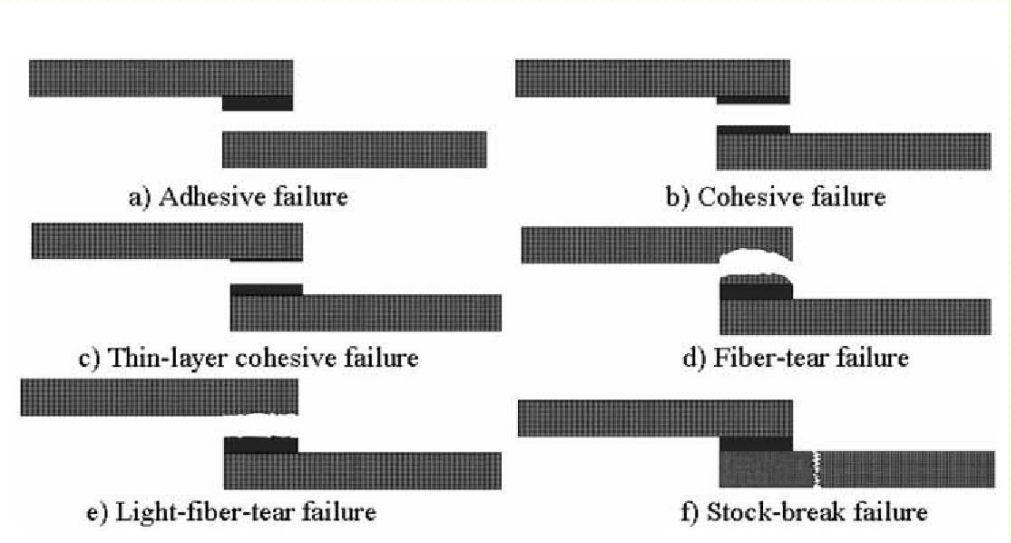

Fig.4 Common Failure modes in lap joints [2]

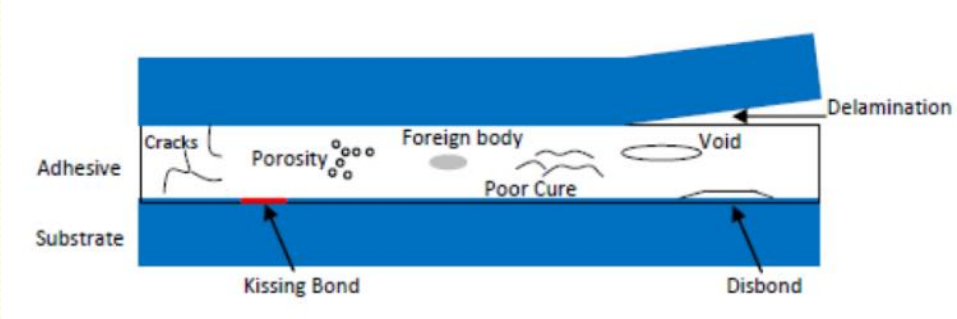

Fig.5 Defects in bonded joints [3]

Motivation

- Previous researches have focused on defects in the bond line [3-10]
- Higher mechanical stresses are observed at the ends of an overlap of single lap adhesive bonded joints.
- Any inclusion present at the ends of the overlap, in the adherents, could increase stresses locally, causing reduction in failure strengths.
- The aim of the current study was to investigate the effect of the position of inclusions present between the first and the second plies of the adherent, from the bond line

Experimental work

Joint Design and Fabrication

1. *Adherent fabrication*
   - Adherents made of Carbon Fiber Reinforced polymer
   - INF Proset 114/211 matrix reinforced with T700 fibers.
   - PTFE strips, 12.7mm wide, inserted in half of the adherents fabricated to emulate an inclusion
   - Inclusion placed between 1st and 2nd plies counted from the bonding surface
   - Curing and heat treatment
   - Adherents cut using circular tile saw

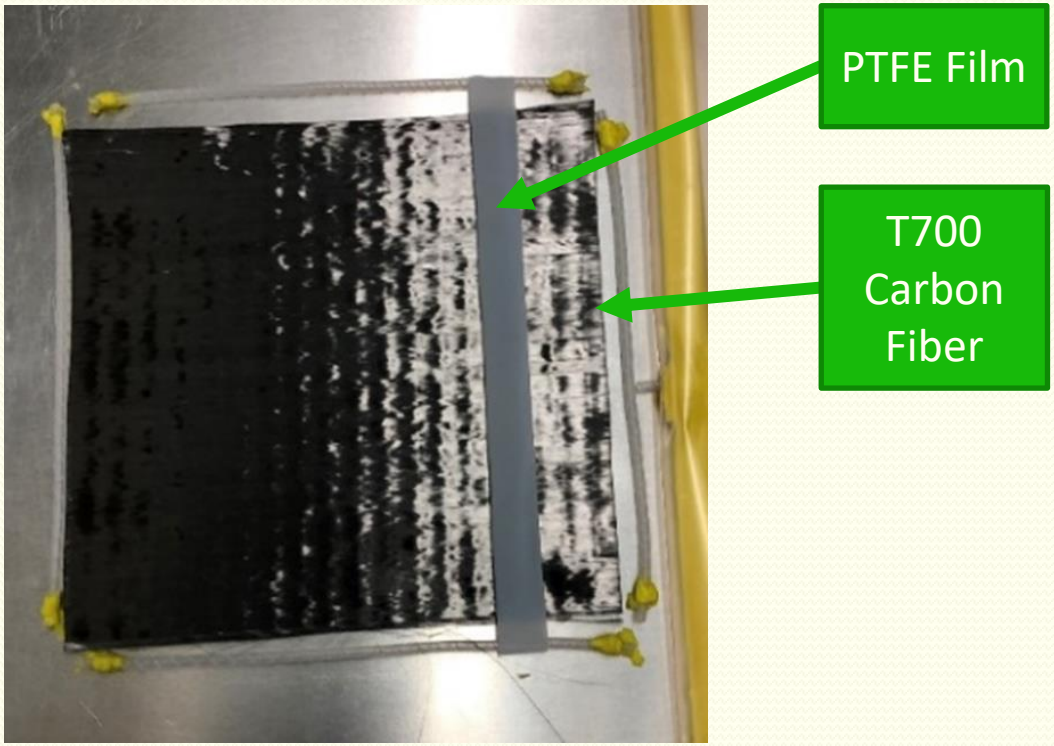

Fig.6 Placement of PTFE inclusion during layup process

Experimental work

2. *Bond fabrication*

- A defective and non defective adherent bonded using Hysol EA 9309 NA epoxy adhesive
- Thickness of 0.254 mm using PTFE strips
- Bonds in SLJ config accordance with ASTM D1002 [11]
- Bond surface preparation
- Overlap length

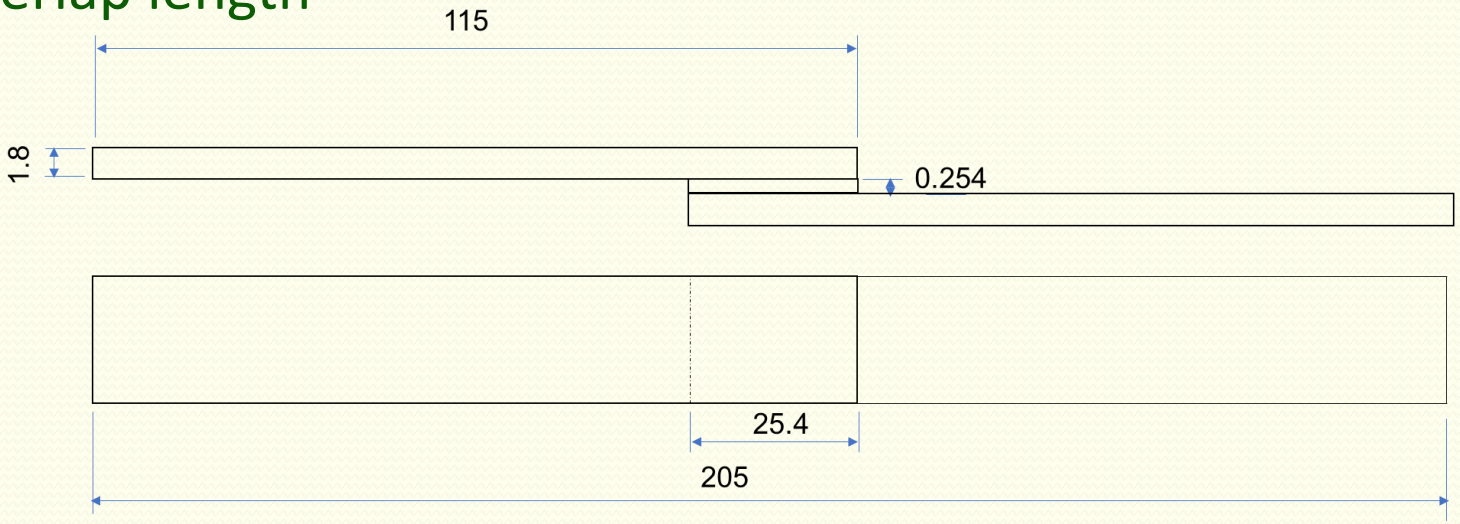

Fig.7 Geometric details of single lap joint configuration (All dimensions in mm)

Experimental work

3. *Experimental plan*

- Position of inclusion varied with respect to the origin
- Three different positions tested

Specimen ID	Position of left end of PTFE inclusion w.r.t origin (x) (mm)
Non-Defective	---
A	0
B	-6.35
C	-12.7

Table.1 Experimental Plan (Position w.r.t origin as shown in Figure.7)

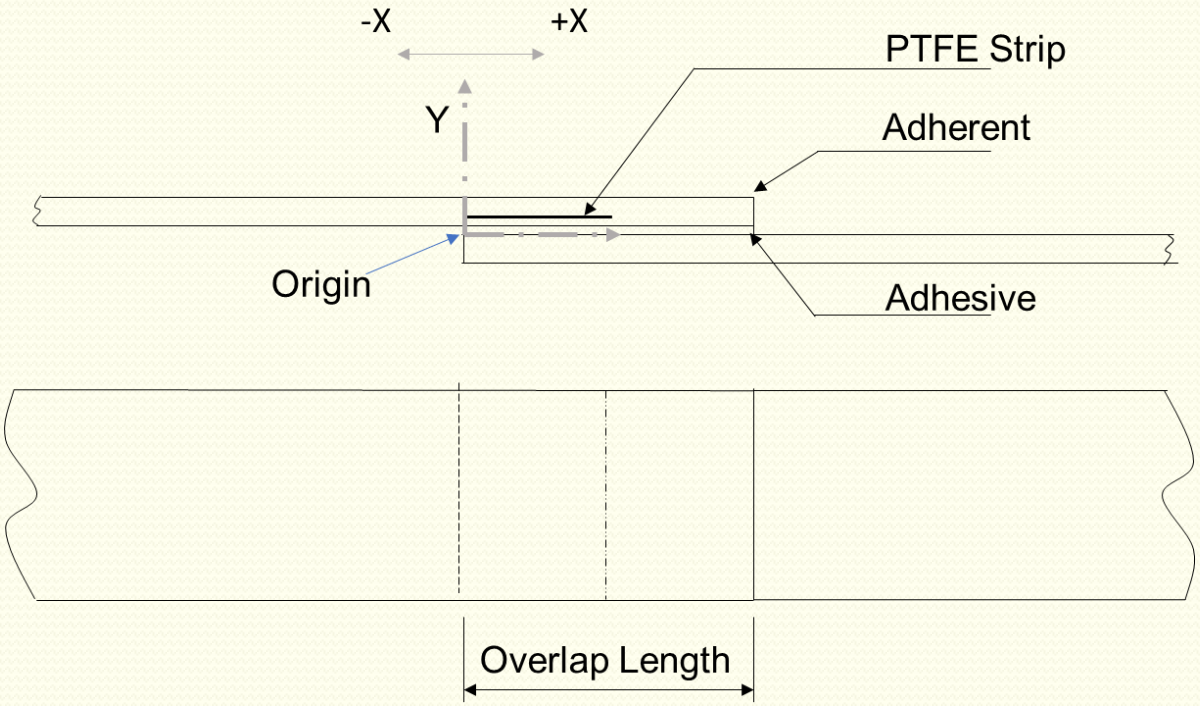

Fig.8 Location of PTFE inclusion in the joint assembly

Experimental work

Materials characterization

- Properties calculated using Tandon Weng method [13]
- Weight of fibers and laminates were recorded to get the mass ratios which were converted to volume fractions

	Elastic Modulus (GPa)	Poisson`s Ratio	Density (g/cc)
Carbon Fiber (T700 UNI)	230	0.2	1.8
Adhesive Hysol 9309 NA	2.331	0.38	1.1
Resin (Proset INF 114/211)	3.36	0.4	1.14

Table.2 Material properties of Carbon fiber [14], resin[15] and the adhesive [12]

	E11 (GPa)	E22 (GPa)	E33 (GPa)	ϑ_{12}	ϑ_{13}	ϑ_{23}	G_{12} (GPa)	G_{13} (GPa)	G_{23} (GPa)
Composite Properties	134.13	12.18	12.18	0.39	0.39	0.57	4.28	4.28	3.68

Table.3 Mechanical properties of carbon fiber adherent calculated using Tandon Weng method [13]

Finite element modeling

- SLJ analyzed in ABAQUS CAE
- CFRP adherents modelled as orthotropic materials
- 2D plane strain elements CPE4 used
- Model created in two parts and joined using tie constraint
- Inclusion modeled as a frictionless contact

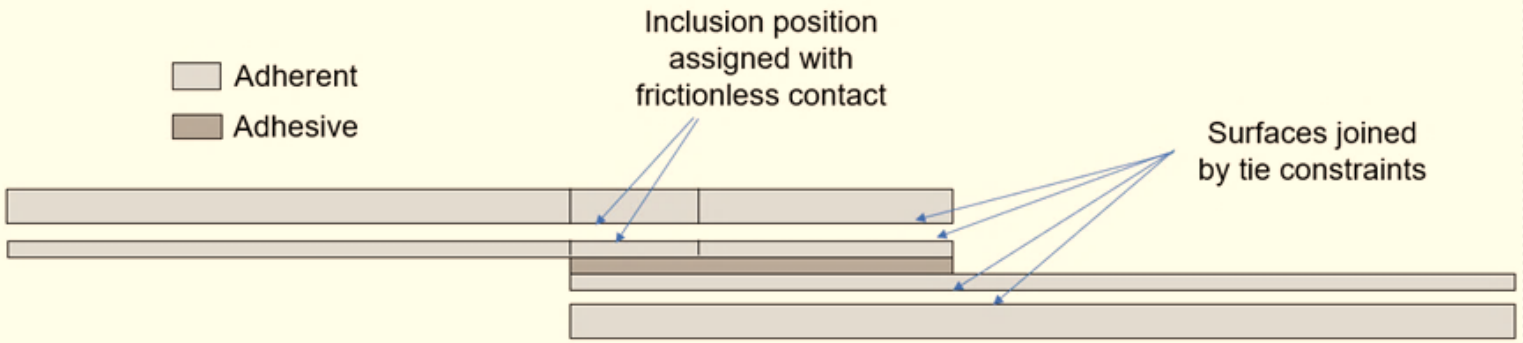

Fig.9 Schematic showing method of assembly of FE model using tie constraints

Results and Discussions

- Adherent failure observed in the first ply adjacent to the bond line
- Lowest failure load for the inclusion position of x = 0 mm
- Inclusion position of x = -12.7 and non-defective joints exhibit similar failure strength
- Stress strain curves have a similar slope

Fig.10 Failed surface for a non-defective joint

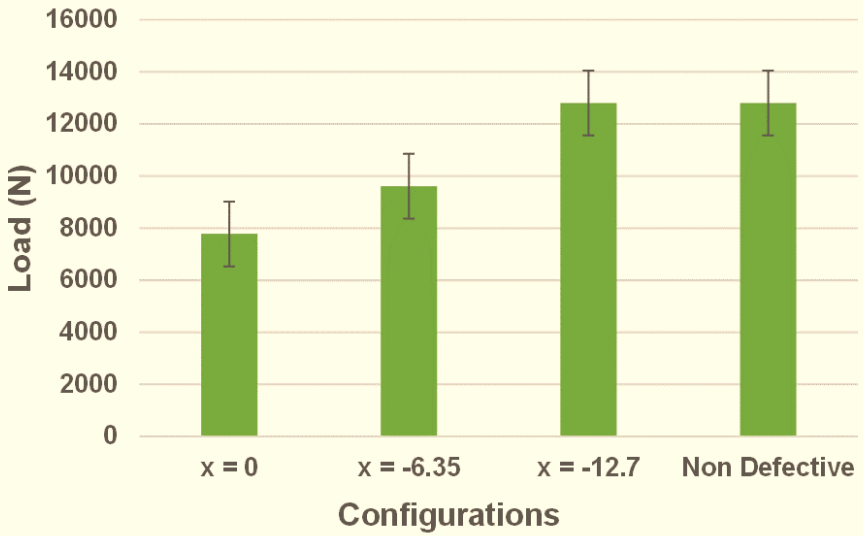

Fig.11 Experimental Load-Displacement (Crosshead) of selected specimen of each configuration

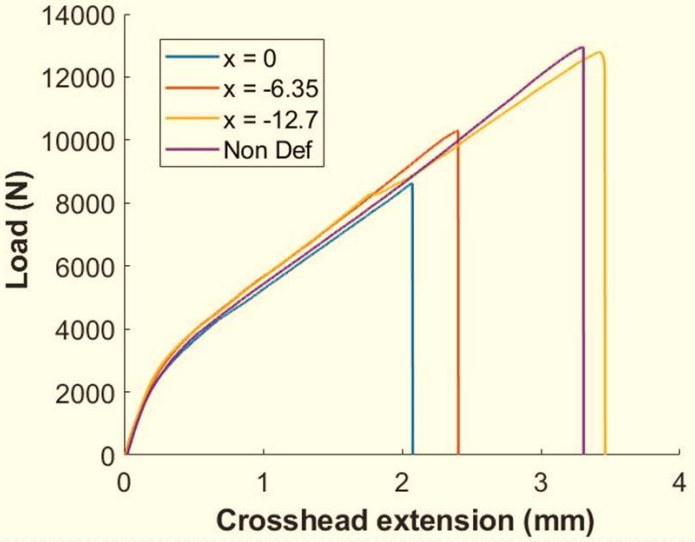

Fig.12 Experimental failure loads for the various configurations

Results and Discussions

- Shear and peel stresses were calculated along a path through the middle of the first ply adjacent to the bond line
- FE model of various inclusion widths showed no dependence of inclusion width on the peak stresses

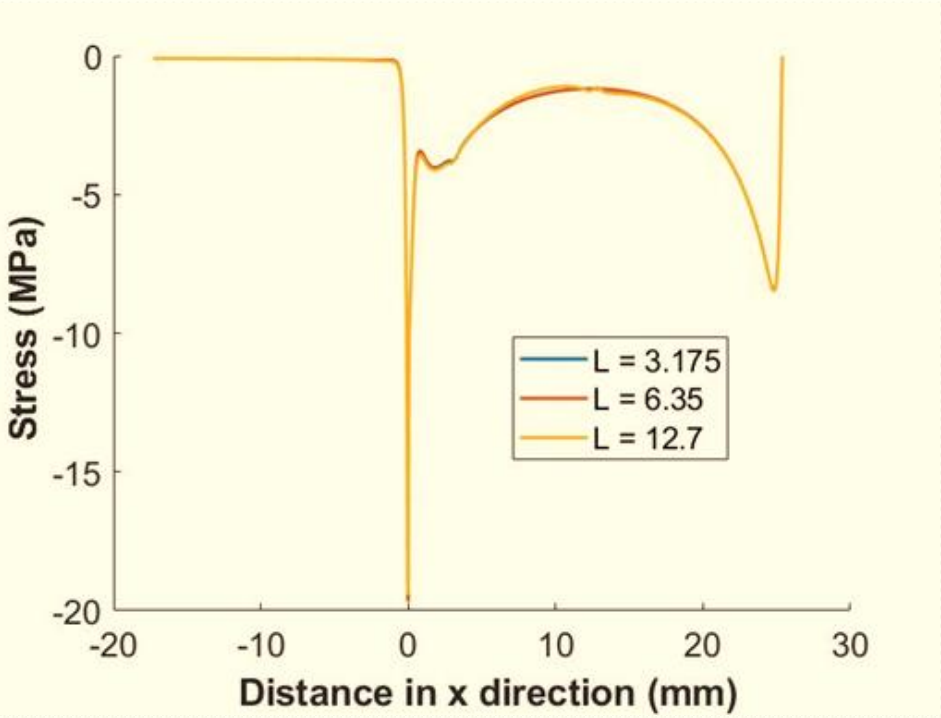

Fig.13 Comparison of Peel stress across mid-ply of first ply counted from the bond line for different lengths of the inclusion, at x=0 (Figure 1a). L indicates the length of the inclusion along the bond line

Results and Discussions

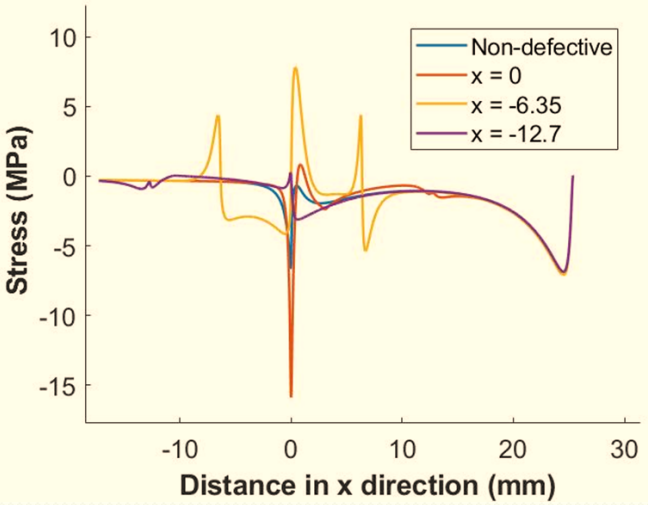

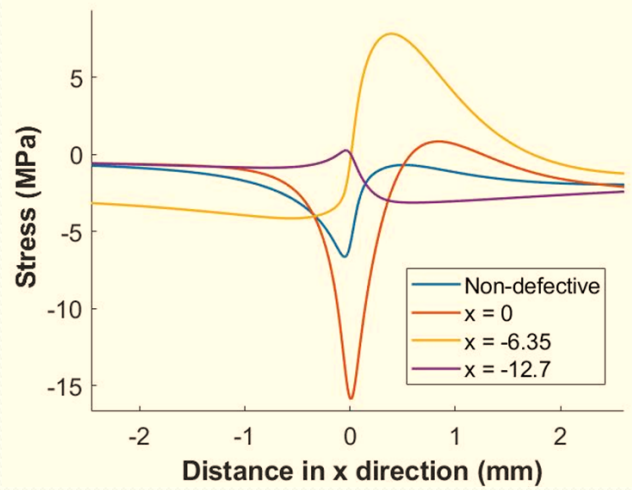

Fig.14
Shear stress distributions in the middle of first ply for various configurations b) magnified view of detail A

Fig.15
a) Peel stress distributions in the middle of first ply for various configurations b) magnified view of detail A

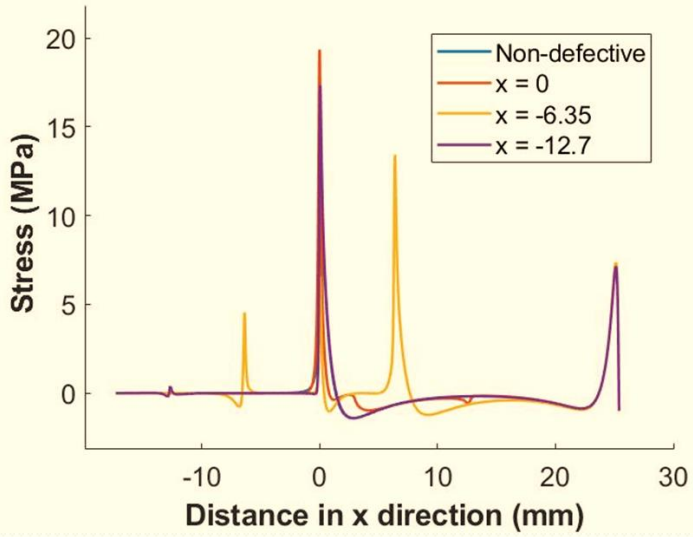

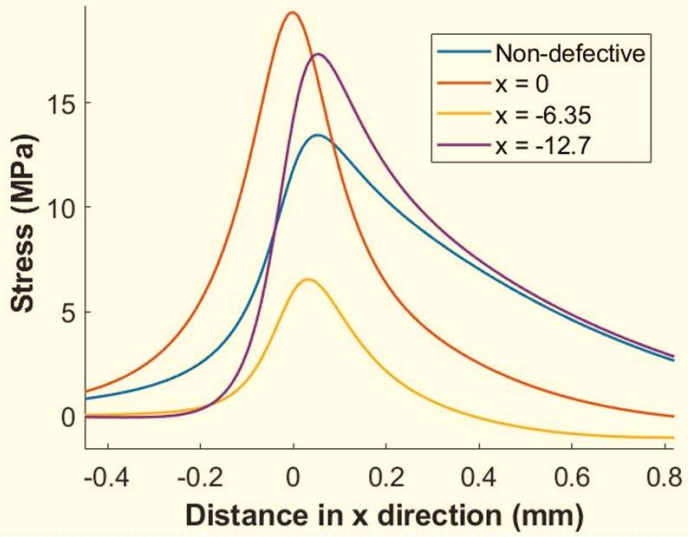

Results and Discussions

- Higher shear stresses in the configurations indicate an effect of higher shear stress on failure load
- Vertical displacement is lowest for position of x = -6.35 mm
- This explains lower peel stress in the position of x = -6.35 mm
- Further investigations would be done along with the application of a suitable failure criteria for a better understanding of the root cause of strength reduction.

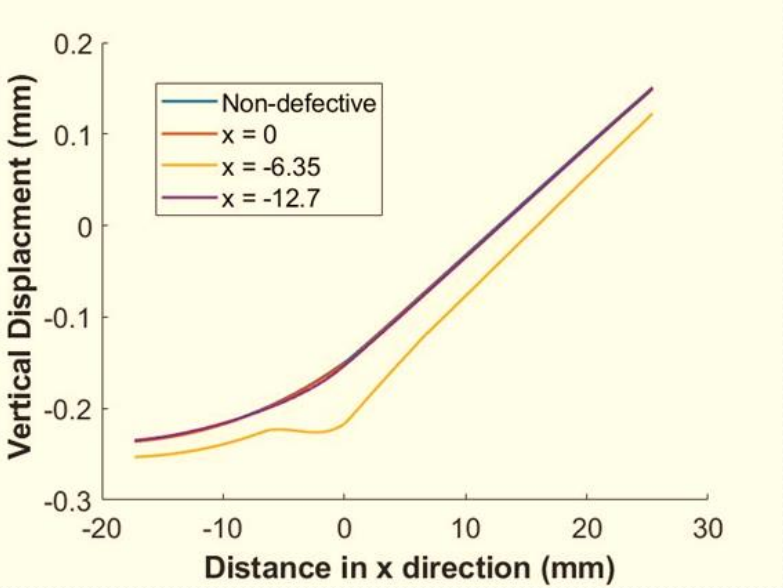

Fig.16 Comparison of vertical displacements (Uy) for various defect positions

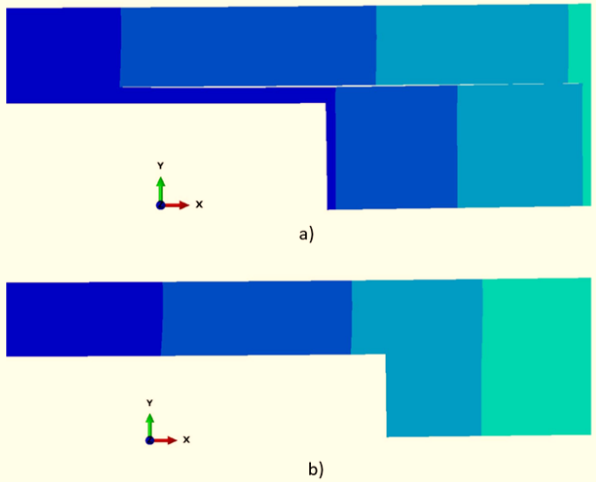

Fig.17 Vertical displacement (Uy) contours for a) Defect position x = -6.35 b) Non-defective joint

Conclusions

1. The position of inclusions present between the first and the second ply counted from the bond line influenced the strength of bonded joints.
2. An inclusion present in the overlap region of a single lap joint, with one of the ends located above the overhang end of the overlap, resulted in lower strengths among all configurations. The shear and peel stresses in the first ply were found to be greater than other configurations which explains the lower strength.
3. An inclusion existing completely outside of the overlap region did not result in significant reduction in failure strength.
4. The size of the inclusion did not influence the stress states of the bonded joints.

Acknowledgements

- Dr. Douglas E Smith
- Dr. David A Jack
- L3 Harris Technologies
- Baylor University

References

1. Obel T, Holzhüter D, Sinapius M, Hühne C. A hybrid bondline concept for bonded composite joints. International Journal of Adhesion and Adhesives 2016;68:229–38. https://doi.org/10.1016/j.ijadhadh.2016.03.025.
2. Banea MD, da Silva LFM. Adhesively bonded joints in composite materials: An overview. Proceedings of the Institution of Mechanical Engineers, Part L: Journal of Materials: Design and Applications 2009;223:1–18. https://doi.org/10.1243/14644207JMDA219.
3. Hart-Smith L. Further Developments in the Design and Analysis of Adhesive-Bonded Structural Joints. In: Kedward K, editor. Joining of Composite Materials, 100 Barr Harbor Drive, PO Box C700, West Conshohocken, PA 19428-2959: ASTM International; 1981, p. 3-3–29. https://doi.org/10.1520/STP33472S.
4. Heslehurst RB. Observations in the structural response of adhesive bondline defects. International Journal of Adhesion and Adhesives 1999;19:133–154.
5. Pereira AB, de Morais AB. Strength of adhesively bonded stainless steel joints. International Journal of Adhesion and Adhesives 2003;23:315–22. https://doi.org/10.1016/S0143-7496(03)00049-6.
6. Ribeiro FL, Borges L, d'Almeida JRM. Numerical stress analysis of carbon-fibre-reinforced epoxy composite single-lap joints. International Journal of Adhesion and Adhesives 2011;31:331–7. https://doi.org/10.1016/j.ijadhadh.2011.01.008.
7. Berry NG, d'Almeida JRM. The influence of circular centered defects on the performance of carbon–epoxy single lap joints. Polymer Testing 2002;21:373–379.
8. You M, Yan Z-M, Zheng X-L, Yu H-Z, Li Z. A numerical and experimental study of gap length on adhesively bonded aluminum double-lap joint. International Journal of Adhesion and Adhesives 2007;27:696–702. https://doi.org/10.1016/j.ijadhadh.2007.02.005.
9. Ribeiro FMF, Campilho RDSG, Carbas RJC, da Silva LFM. Strength and damage growth in composite bonded joints with defects. Composites Part B: Engineering 2016;100:91–100. https://doi.org/10.1016/j.compositesb.2016.06.060.

References

10. Takeda N, Minakuchi S. Optical fiber sensor based life cycling monitoring and quality assessment of carbon fiber reinforced polymer matrix composite structures. 2017 25th Optical Fiber Sensors Conference (OFS), 2017, p. 1–4. https://doi.org/10.1117/12.2272472.
11. D14 Committee. Test Method for Apparent Shear Strength of Single-Lap-Joint Adhesively Bonded Metal Specimens by Tension Loading (Metal-to-Metal). ASTM International; n.d. https://doi.org/10.1520/D1002-10.
12. LOCTITE EA 9309NA AERO.pdf n.d. https://tdsna.henkel.com/americas/na/adhesives/hnauttds.nsf/web/D0FB023C08D81E1E85257CD60065C913/$File/LOCTITE%20EA%209309NA%20AERO.pdf (accessed May 21, 2020).
13. Tucker III CL, Liang E. Stiffness predictions for unidirectional short-fiber composites: Review and evaluation. Composites Science and Technology 1999;59:655–71. https://doi.org/10.1016/S0266-3538(98)00120-1.
14. Toray Composites T700 carbon fiber technical data sheet n.d. https://www.toraycma.com/ (accessed May 21, 2020).
15. Infusion epoxies PRO-SET. Https://WwwProsetepoxyCom/ n.d.
16. 3D Design & Engineering Software - Dassault Systèmes®. Vélizy-Villacoublay, France: n.d.

Questions